

•水利与土木工程•

DOI:10.12454/j.jsuese.202500038



本刊网刊

环境温度对钢管约束混凝土柱抗震性能影响机理试验

王力¹, 胡琦¹, 潘启仁¹, 顾皓玮¹, 翟启远², 虞庐松¹, 亢二聪³

(1. 兰州交通大学 土木工程学院, 甘肃 兰州 730070; 2. 山西交院试验检测有限公司, 山西 太原 030000; 3. 天津大学 建筑工程学院, 天津 300350)

摘要:为研究环境温度对钢管约束混凝土柱抗震性能的影响机理,开展了不同环境温度(-40、20、60 °C)下9组钢管约束混凝土柱的拟静力试验,通过分析各试件的破坏形态、水平承载力、刚度退化、耗能能力等指标,揭示了环境温度对钢管约束混凝土柱抗震性能的影响机理;并根据试验结果,提出了考虑环境温度影响的钢管约束混凝土柱水平承载力计算公式。结果表明:1)钢管约束混凝土柱的材料特性及钢-混接触面黏结性能随环境温度的改变而改变,相比于常温工况,高温、低温工况下的试件延性均呈不同幅度下降,但下降的机理并不相同;2)高温(60 °C)工况下,由于混凝土强度与钢-混凝土界面黏结强度均降低,导致试件水平承载力和延性系数分别最大降低了4.25%和5.27%;3)低温(-40 °C)工况下,由于试件材料强度提高,以及温度附加套箍效应的作用,试件水平承载力最大提高了20.88%,但延性系数降低了37.52%。提出的考虑环境温度影响的钢管约束混凝土柱水平承载力计算修正公式具有较好的可靠性和准确性,可为高寒地区钢管约束混凝土结构的设计提供必要依据。

关键词:钢管约束混凝土柱;环境温度;拟静力试验;抗震性能;水平承载力;温度附加套箍效应

中图分类号:U448

文献标志码:A

文章编号:2096-3246(2026)02-0203-12

钢管约束混凝土(steel tube confined concrete, STCC)是在钢管内填充混凝土,钢管不直接承担纵向荷载,仅对核心混凝土起约束作用的一种组合结构。相较于传统钢管混凝土柱,钢管约束混凝土柱不仅保持了传统组合柱在静力、抗震和抗火等方面的优势,并且由于钢管约束混凝土柱中钢管不直接承受外荷载,能避免钢管发生屈曲,有效降低设计与施工难度,因此在中国的工程建设中得到了广泛应用^[1]。随着新时代西部大开发战略不断推进,这类结构在西北高寒、高烈度地区的应用前景尤为广阔。

中国西北地区年温差大,冬季严寒、干燥,而夏季高温、热辐射强,同时,由于地壳板块运动的影响,地震活动频繁^[2]。钢管约束混凝土柱利用薄壁钢管对核心混凝土提供主动约束的特点,在高寒地区的应用有显著优势和广阔前景。对于钢管约束混凝土结构,钢管与核心混凝土之间的协同作用是保证其力学性能的关键^[3-5]。已有研究表明,环境温度对钢管和混凝土

的材料性能影响显著:低温环境下由于温度附加套箍效应的作用会使约束作用增强;高温环境下钢-混凝土界面可能会发生脱黏滑移、脱空行为。

目前,国内外学者针对钢管约束混凝土柱抗震性能的研究主要集中于截面形状、内置钢筋/型钢、柱-RC梁框架结构/节点、材料性能、加固等方面。王秋维^[6-7]、戴岩^[8]、聂少锋^[9]、刘坚^[10]等通过开展试验及有限元分析,分别采用布置阻尼器,内置型钢、环梁、外套管等对钢管约束混凝土柱节点进行增强、保护,并开展参数分析,给出了各种形式对节点保护的优势所在。Bu^[11]和周绪红^[12]等通过试验和数值分析,对钢管约束钢筋自应力混凝土柱和钢管约束型钢高强混凝土柱抗震性能进行研究,分析了轴压比、径厚比、长细比等参数对试件抗震性能的影响。臧兴震^[13]、Xu^[14]、Chen^[15]、Feng^[16]等采用外包钢管、FRP对钢管约束混凝土柱进行约束加固,分析了各参数对构件的影响,为该种加固方式的应用提供依据。欧智菁^[17]、王宇航^[18]等分别对钢管约束混

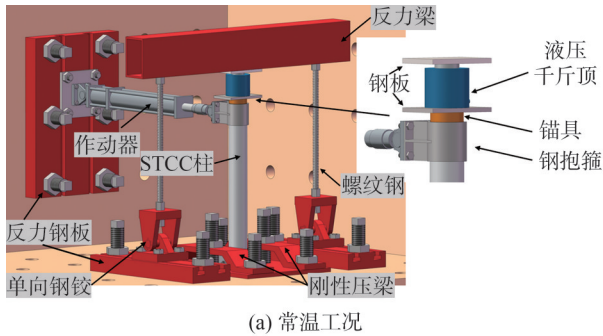
收稿日期:2025-01-17 修回日期:2025-04-24 网络出版日期:2025-06-10

基金项目:国家自然科学基金项目(52268027);甘肃省自然科学基金青年项目(25JRRA207);甘肃省联合科研基金重点项目(24JRRA869);山西交通控股集团科技创新项目(23-JKKJ-6)

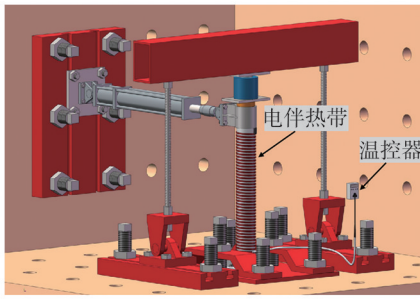
作者简介:王力(1993—),男,副教授,博士。研究方向:寒区组合结构抗震。E-mail:wangli1993@mail.lzjtu.cn

1.3 加载装置及试验温控装置

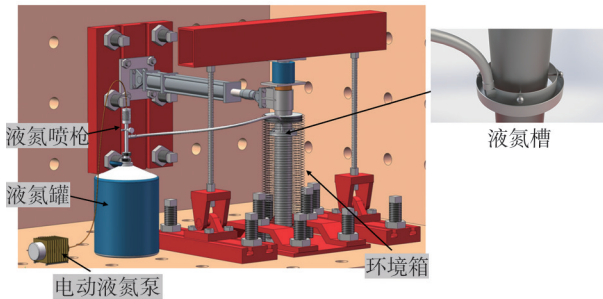
为了保证在开展不同环境温度试验时试件恒温,自主开发了常温、低温和高温工况试验装置,加载装置示意图见图2。整个加载系统由水平向加载装置与竖向加载装置组成,水平往复荷载与竖向恒定荷载分别通过电液伺服作动器和100 t千斤顶进行施加,如图2(a)所示。底部限位钢板与两块刚性压梁通过6根锚杆固定后形成柱底限位装置,试件与底部限位钢板通过8个高强螺栓连接,柱顶与作动器通过特制的钢抱箍进行连接。采用反力梁施加柱轴力,该装置的优势在于其底部转动铰的存在,使得反力梁位置在加载过程中可以跟随柱顶位置的变化而变化,确保千斤顶与柱顶始终保持竖直,竖向力更加稳定。在千斤顶与核心混凝土之间,放置有锚具与混凝土接触,锚具上放有钢垫板与千斤顶底部接触,以实现仅核心混凝土承受竖向力。



(a) 常温工况



(b) 高温工况



(c) 低温工况

图2 试验加载装置示意图

Fig. 2 Schematic diagram of test loading device

对于高温(60 °C)工况试验,在钢管外壁螺旋缠绕电伴热带加热升温至试件目标温度,恒温24 h,然后,采用自控温系统,使其温度保持在目标温度 ± 1 °C范围内,

见图2(b)。低温(-40 °C)工况试验是将试件置于超低温试验箱中降温,降至目标温度后恒温保持24 h。试验过程中的保温装置由YDS-50B-210液氮罐、电动液氮泵、液氮槽与环境箱4个主要部分构成,见图2(c)。环境箱壁采用PU聚氨酯铜丝软管,其可伸缩透明的特点可以满足试验往复加载的加载模式;将特制里高外低的液氮槽固定在钢管上部,液氮泵将液氮喷到液氮槽中。待试验准备工作完成后,向保温箱中匀速通入液氮,利用常压下氮的沸点为-196.56 °C的物理性质,使环境箱内温度恒定在目标温度附近。钢管约束混凝土柱表面、核心混凝土内部和环境箱内部均设置有PT100温度传感器,实时检测试件表面及保温箱内温度。

1.4 加载制度

正式加载前,首先施加10%设计压力值对核心混凝土进行预压,消除千斤顶和核心混凝土之间空隙。正式试验时,将千斤顶加载至设计轴力并保持恒定不变,然后施加水平往复荷载。采用位移加载控制方式,根据《建筑抗震试验规程》(JGJ/T 101—2015)^[37],控制方式为变幅位移与等幅位移混合控制。加载制度如图3所示。当侧移率分别为 $\pm 0.25\%$ 、 $\pm 0.5\%$ 、 $\pm 0.75\%$ 时,每级加载循环1次;当侧移率在 $\pm 1.0\%$ ~ $\pm 4.0\%$ 之间时,每级加载循环3次。当侧移率在 $\pm 1.0\%$ ~ $\pm 2.0\%$ 之间时,加载位移步为5 mm;当侧移率在 $\pm 2.0\%$ ~ $\pm 4.0\%$ 之间时,加载位移步为10 mm。加载侧移率为 $\pm 5.0\%$ 及以上,每级加载循环2次,加载位移步为10 mm。当水平荷载下降至峰值荷载的85%或当钢管发生断裂时停止加载,试验结束。

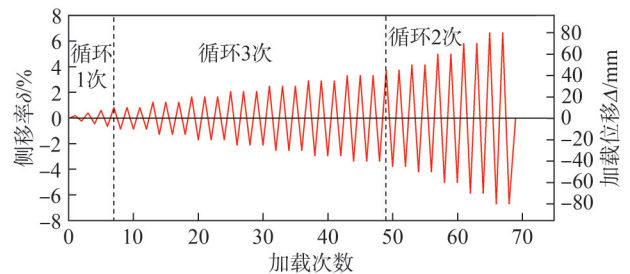


图3 加载制度

Fig. 3 Test loading system

2 试验过程和破坏现象

各试件在加载结束后的破坏形态如图4所示,试验结束后可以观察到同一温度工况下试件破坏形态相似,表现为典型的压弯塑性铰破坏。各温度工况下,试件底部鼓曲位置为加劲肋上方10~30 mm处,由加载初期的局部鼓曲逐渐向两侧发展。混凝土强度越高,试件底部的加劲肋上方的局部鼓曲越明显。此外,各工况下,试件均表现为钢管撕裂破坏,高温和常温工况下,钢管撕裂位置位于鼓曲的中部,低温工况下钢管则沿

着鼓曲的下侧开裂,这是由于低温环境下混凝土强度大幅增大导致。试件的破坏过程大致分为弹性变形阶段、弹塑性变形阶段以及破坏阶段。

1)弹性变形阶段:钢管与核心混凝土受力变形稳定,力随位移增长速度较快,柱身没有发生明显变化。

2)弹塑性变形阶段:当水平位移加载至 20 mm(初始屈服位移),试件开始进入弹塑性变形阶段,观察到钢管局部出现轻微鼓曲,局部屈曲大致出现在加劲肋上方 20 mm 处。核心混凝土对外钢管具有支撑作用,有效抑制了钢管向内凹陷的趋势。随着水平位移加载至 40 mm,钢管鼓曲明显,在加载过程中观察发现,向

外变形首先发生在垂直于加载方向两侧的加劲肋上方,并按一定坡度逐渐斜向下扩展到平行于加载方向没有加劲肋的两侧,这是由于试件在其底部鼓曲位置处形成塑性铰,核心混凝土断裂位置形成一个球面,压溃的混凝土挤压钢管,导致最早出现鼓曲的位置向两侧发展时按一定斜度扩展延伸。最后,在弹塑性阶段结束时,试件达到了水平峰值荷载。

3)破坏阶段:在水平位移加载至 80 mm(4倍屈服位移)的过程中,由于试件底部出现严重破坏,随着加载位移的增大,水平荷载下降,钢管底部裂缝加速扩展,直至柱底完全断裂,试件被破坏。

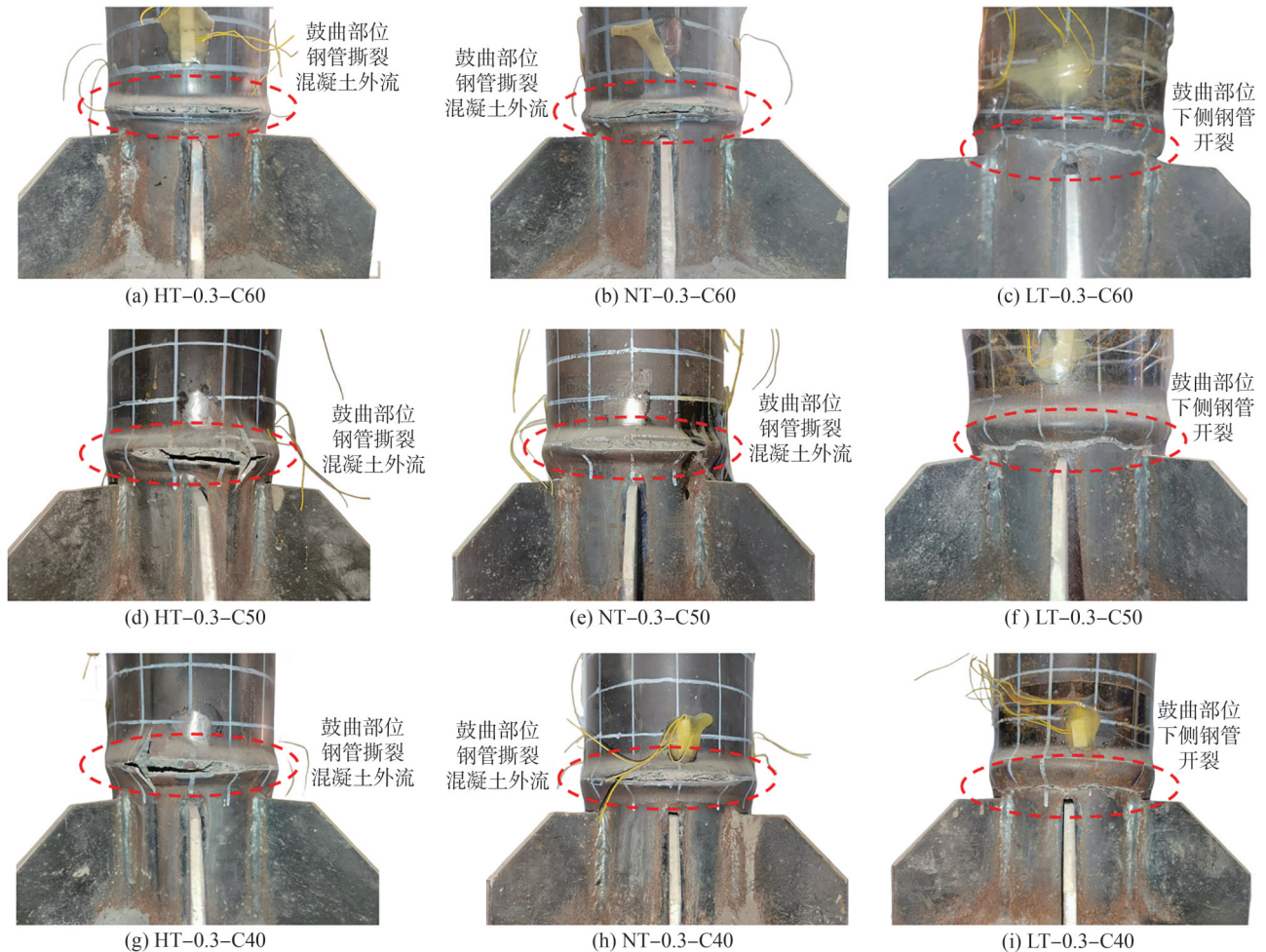


图4 试件加载后的破坏形态

Fig. 4 Failure modes of the specimens after loading

3 试验结果分析

3.1 滞回曲线

各试件滞回曲线如图5所示。图5中, P 为水平荷载, Δ 为加载位移。

由图5可知,各试件的滞回曲线整体呈现梭形,形状较为饱满,没有明显的捏缩现象,表明各工况下钢管约束混凝土柱均有良好的抗震性能。各试件的变形

过程基本一致,在加载初期,试件处于弹性变形阶段,刚度无明显变化,曲线基本呈线性发展,残余变形几乎为0;随着位移增加,柱底塑性铰开始形成,滞回曲线略微波动,开始鼓曲。进入弹塑性变形阶段后,试件开始出现残余位移,并不断增大,强度和刚度逐级退化,荷载提升的幅度逐渐缓慢,滞回环面积不断增大且趋于饱满;达到水平峰值荷载后,曲线开始呈现下降趋势,出现轻微捏缩。

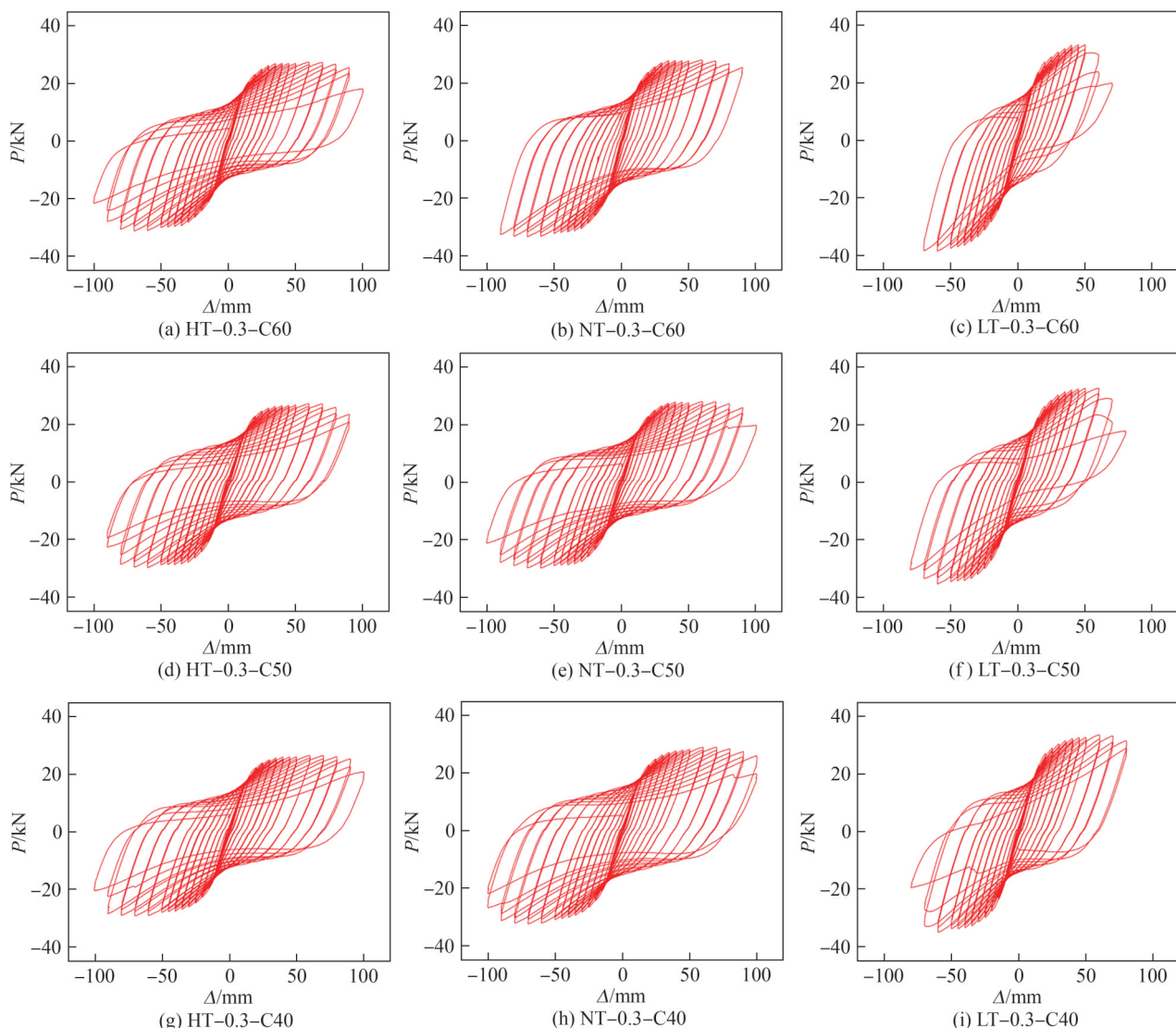


图5 试件水平荷载-位移滞回曲线

Fig. 5 Load-displacement hysteretic curves of specimens

相较于常温工况,在高温工况下,由于钢材和混凝土的热力学性能差异显著,钢管膨胀变形比混凝土膨胀变形要大,约束作用减弱,试件承载力下降。低温工况下,材料性能提升的同时,钢管收缩程度比混凝土收缩程度大,温度附加套箍效应作用、约束作用进一步增强,试件承载力提高。随着混凝土强度的增大,试件峰值承载力有所增大,滞回环更加饱满,极限变形增大,耗能更好。总体来看,其他参数相同的条件下,混凝土强度对钢管约束混凝土柱的抗震性能的影响不大。

3.2 骨架曲线

将滞回曲线的每级位移第一圈峰值点荷载连线作为骨架曲线,得到水平荷载-位移($P-\Delta$)骨架曲线,如图6所示。

由图6(a)~(c)可知,相同混凝土强度下,随着温度的降低,钢管约束混凝土柱骨架曲线初始斜率增

大,说明钢管约束混凝土柱的初始刚度有所增大。相较于常温工况,低温($-40\text{ }^{\circ}\text{C}$)工况下试件初始刚度最大提高了16.23%,屈服荷载和峰值荷载分别平均提高了20.43%和20.88%;高温($60\text{ }^{\circ}\text{C}$)工况下试件初始刚度最大降低了12.52%,试件屈服荷载和峰值荷载分别平均下降了3.61%和4.25%。究其原因,混凝土与钢材的弹性模量、钢材的屈服强度与温度均存在负相关关系,且低温下钢管变形程度比混凝土变形程度要大,引起附加套箍效应,致使低温下试件的初始刚度与水平承载力高于常温工况;而在高温工况下,高温混凝土内部水分蒸发、粗骨料膨胀,致使混凝土内部孔隙率增大,导致核心混凝土弹性模量减小,同时高温还会加速试件内部微裂缝的发展,承载力增速也相对较慢。

由图6(d)~(f)可知,在其他条件相同的情况下,不同混凝土强度的钢管约束混凝土柱的骨架曲线

弹性变形阶段基本重合。随着混凝土强度的增大,试件初始刚度和水平承载力有所提高,但水平承载力提高幅度较小。混凝土强度等级从C40增至C60时,试件

初始刚度、屈服荷载和峰值荷载分别最多提高19.19%、6.79%和7.70%。总体来看,不同混凝土强度的钢管约束混凝土柱的抗震性能相对接近。

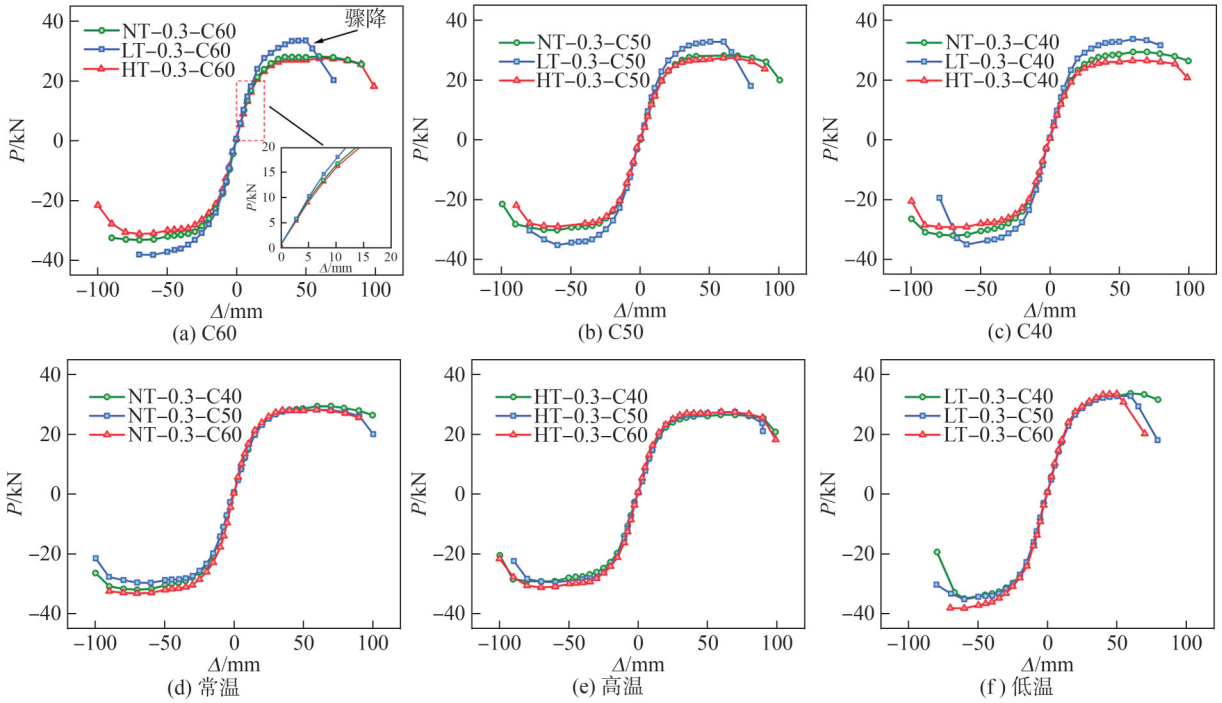


图 6 试件骨架曲线

Fig. 6 Comparison of skeleton curves of specimens

3.3 延性性能

屈服力 P_y 和屈服位移 Δ_y 采用等效能量法^[38]确定,原理如图7所示。 BYM 和 OAB 有相同的面积。随后,从 Y 点开始画一条垂线,与骨架曲线相交于 C 点,即为屈服点。试件的位移延性系数 μ 计算公式为 $\mu = \Delta_u / \Delta_y$,其中: Δ_y 为能量等值法得到的屈服位移; Δ_u 为极限位移,对应峰值荷载 P_m 降至85%时的位移值。图7中, P_y 、 P_u 分别为 Δ_y 、 Δ_u 对应的荷载值, Δ_m 为 P_m 对应的位移值。位移延性系数如表3所示。

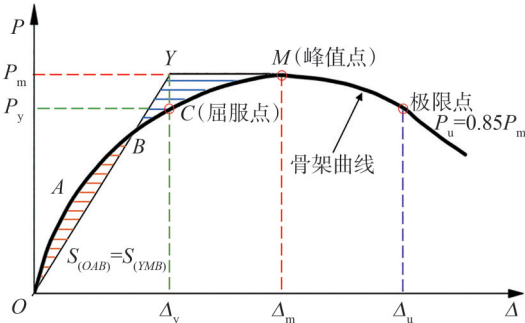


图 7 等效能量法和特征点定义示意图

Fig. 7 Schematic diagram of equivalent energy method and definition of feature points

由表3可知,常温下试件的延性系数均大于3.0,表现出良好的变形能力。相较常温工况,低温(-40℃)工况下,位移延性系数最大减小了37.52%,这是由于混

土材料的脆性增强,核心混凝土的累积损伤显著增大,钢管约束混凝土柱在弹塑性变形阶段的塑性发展受到限制,导致钢管约束混凝土柱在达到峰值承载力后,其承载力的降低速度相对较快,试件延性变差。高温工况下,位移延性系数最大减小了5.27%,这是因为高温下钢材弹性模量降低,混凝土抗压强度降低,钢管对混凝土约束作用减弱,以及钢-混凝土界面局部发生脱黏滑移、脱空行为^[5],钢管对核心混凝土柱的约束效应减弱,导致结构刚度下降,承载力与延性降低。

3.4 刚度退化

采用割线刚度来表示反复荷载作用试件的刚度退化。割线刚度表达式为:

$$K_i = \frac{|+F_i| + |-F_i|}{|+X_i| + |-X_i|} \quad (1)$$

式中, K_i 为试件第 i 次的割线刚度, $+F_i$ 和 $-F_i$ 分别表示正、负向第 i 级加载时首圈滞回环的峰值力, $+X_i$ 和 $-X_i$ 分别表示正、负向第 i 级加载时首圈滞回环峰值力对应的位移值。各构件的刚度退化的关系曲线如图8所示。

由图8可知,各试件的刚度退化过程相似,均表现为先快后慢。常温工况下,钢管约束混凝土柱的刚度退化曲线没有发生突变,下降得相对平缓;而低温工况下,由于核心混凝土和钢管的脆性增大,在往复加载过程中,试件的累积损伤较大,核心混凝土内部因

表3 试件各特征点荷载-位移实测值
Tab. 3 Measured loads and displacements at characteristic points

| 试件编号 | 加载方向 | 屈服点 | | 峰值点 | | 极限点 | | μ | μ 平均值 |
|------------|------|----------|---------------|----------|---------------|----------|---------------|-------|-----------|
| | | P_y/kN | Δ_y/mm | P_m/kN | Δ_m/mm | P_u/kN | Δ_u/mm | | |
| HT-0.3-C60 | 正向 | 24.125 | 22.381 | 27.500 | 59.820 | 23.375 | 92.440 | 4.130 | 3.769 |
| | 负向 | 27.128 | 26.975 | 31.200 | 69.920 | 26.520 | 91.905 | 3.407 | |
| NT-0.3-C60 | 正向 | 24.526 | 21.426 | 28.200 | 59.360 | 25.600 | 89.950 | 4.198 | 3.819 |
| | 负向 | 28.954 | 26.129 | 33.200 | 69.940 | 32.500 | 89.880 | 3.440 | |
| LT-0.3-C60 | 正向 | 29.046 | 24.117 | 33.500 | 49.900 | 28.475 | 58.156 | 2.406 | 2.386 |
| | 负向 | 33.038 | 29.615 | 38.200 | 59.980 | 38.100 | 70.080 | 2.366 | |
| HT-0.3-C50 | 正向 | 24.570 | 24.143 | 27.400 | 59.560 | 23.290 | 89.487 | 3.707 | 3.508 |
| | 负向 | 26.426 | 25.758 | 29.500 | 59.620 | 25.075 | 85.244 | 3.309 | |
| NT-0.3-C50 | 正向 | 24.757 | 23.882 | 28.200 | 60.040 | 23.970 | 93.724 | 3.924 | 3.703 |
| | 负向 | 26.391 | 26.880 | 29.700 | 60.040 | 25.245 | 93.608 | 3.482 | |
| LT-0.3-C50 | 正向 | 28.648 | 24.860 | 32.800 | 50.100 | 27.880 | 67.199 | 2.703 | 2.789 |
| | 负向 | 31.014 | 27.842 | 35.200 | 59.900 | 30.300 | 80.020 | 2.874 | |
| HT-0.3-C40 | 正向 | 23.533 | 23.502 | 26.500 | 59.380 | 22.525 | 95.573 | 4.066 | 3.715 |
| | 负向 | 25.626 | 28.120 | 29.200 | 70.040 | 24.820 | 94.580 | 3.363 | |
| NT-0.3-C40 | 正向 | 25.891 | 26.934 | 29.400 | 59.840 | 26.400 | 99.760 | 3.704 | 3.476 |
| | 负向 | 27.950 | 30.183 | 32.000 | 69.760 | 27.200 | 97.993 | 3.247 | |
| LT-0.3-C40 | 正向 | 29.520 | 26.380 | 33.700 | 59.760 | 31.600 | 79.540 | 3.015 | 2.782 |
| | 负向 | 30.557 | 27.414 | 35.000 | 60.040 | 29.750 | 69.880 | 2.549 | |

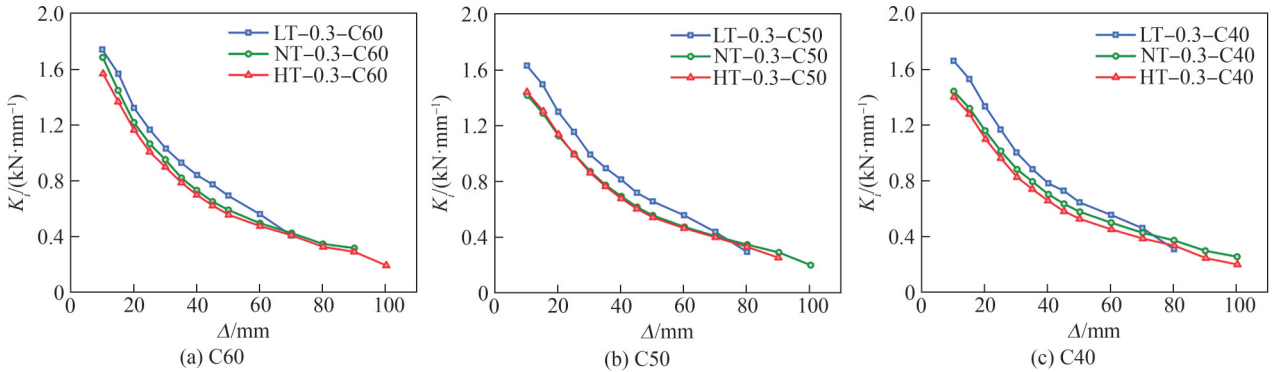


图8 试件刚度退化曲线

Fig. 8 Stiffness degradation curves of specimens

裂缝扩展而被切断后,实际能继续传递和承受力的那部分材料的面积不断缩减,导致试件损伤加剧,刚度退化速率更快,退化程度更深。高温工况下,混凝土中的粗骨料膨胀,内部自由水蒸发,孔隙增加,导致混凝土结构变疏松,刚度显著下降,钢材的屈服强度和弹性模量随温度的升高而降低,相比于常温工况,高温下试件的初始刚度略低,但总体上看,刚度退化速率并无明显改变。

3.5 耗能能力

为评估试件的耗能性能,将累积耗能 E_p 和等效黏滞阻尼系数 ζ_{eq} 作为主要评判指标。等效黏滞阻尼系数采用规范^[37]中的定义按下式进行计算:

$$\zeta_{eq} = \frac{S_{(ABC+CDE)}}{2\pi \cdot S_{(OBF+ODG)}} \quad (2)$$

式中, S 为几何区域面积,计算简图如图9所示。各试件的累计耗能和黏滞阻尼系数对比分别见图10、11。

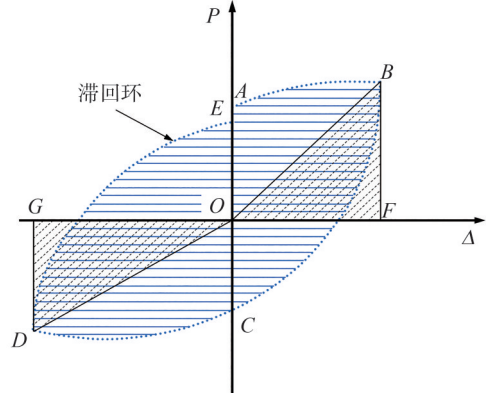


图9 等效黏滞阻尼系数计算简图

Fig. 9 Calculation diagram of equivalent viscous damping coefficient

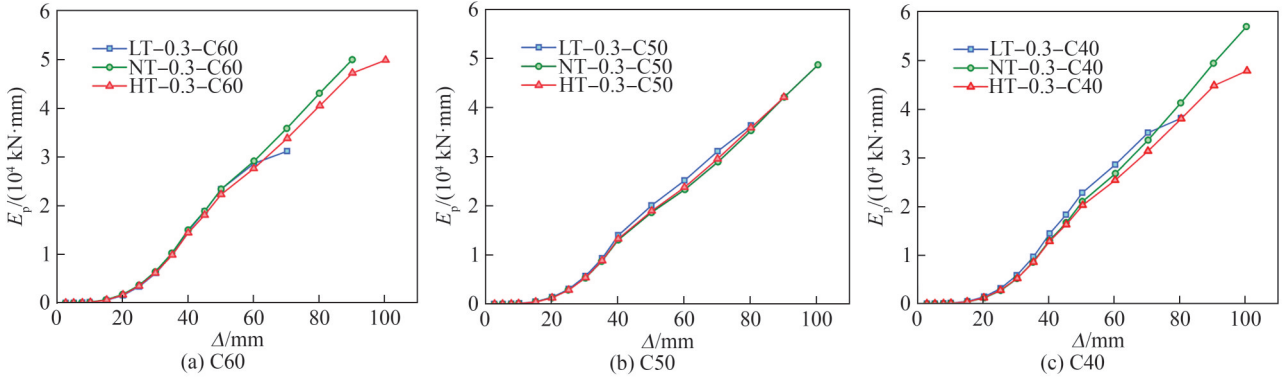


图 10 累积耗能曲线

Fig. 10 Cumulative energy dissipation curves

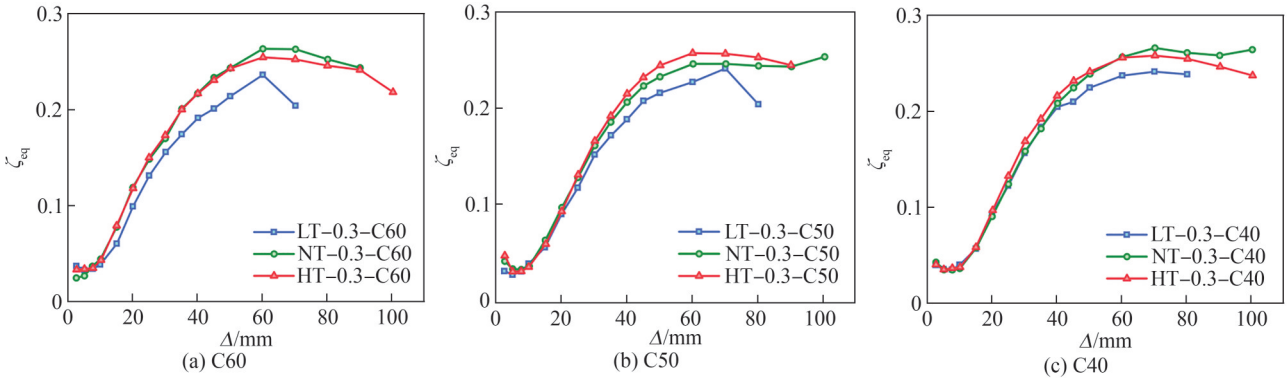


图 11 等效黏滞阻尼系数对比曲线

Fig. 11 Comparing curves of equivalent viscous damping coefficients

由图 10 和 11 可知,随着水平位移的增大,试件累积耗能和等效黏滞阻尼系数增大。

相对于常温工况,低温工况($-40\text{ }^{\circ}\text{C}$)试件在相同位移下,累积耗能增大,但在加载后期,由于低温试件过早发生脆性破坏,其加载结束后的累计耗能要远小于常温试件。高温工况($60\text{ }^{\circ}\text{C}$)下,由于试件水平荷载减小,试件每级循环荷载形成的滞回环面积变小,累积耗能有所减小。对于等效黏滞阻尼系数,低温工况下,等效黏滞阻尼系数较小,表明试件的耗能能力有所降低;高温工况下,试件的等效黏滞阻尼系数有一定变化,但变化幅度不大,表明高温($60\text{ }^{\circ}\text{C}$)对试件的耗能能力影响不大。

4 水平承载力计算公式修正

研究^[39]表明,常温工况下钢管约束混凝土水平承载力一般满足下式:

$$P_u = \frac{(1 - 0.15n_0)M_u}{l - D/2} \quad (3)$$

式中: P_u 为极限水平承载力,根据文献[40]求解; l 为试件计算高度,本文取 $1\ 020\text{ mm}$; D 为钢管直径; M_u 为截面极限抗弯承载力; n_0 为实际轴压比。

环境温度引起的材料变异性 and 温度附加套箍效应是导致钢管约束混凝土柱水平承载力变化的主要

原因。由于环境温度对钢管约束混凝土柱影响的复杂性,且与多参数相关,因此本文采取拟合的方式来考虑其影响。为便于分析环境温度对钢管约束混凝土试件水平承载力的影响规律,定义试件水平承载力影响系数为 k_0 ,计算如下:

$$k_0 = \frac{P_u(T)}{P_u} \quad (4)$$

式中, T 为构件实际所处的环境温度, $P_u(T)$ 为考虑环境温度不同工况下钢管约束混凝土柱水平承载力试验值。

基于试验结果,通过回归拟合出水平承载力影响系数 k_0 的表达式如下:

$$k_0 = 2 \times 10^{-5}T^2 - 0.0025T + 1.1099 \quad (5)$$

将式(4)代入式(3),可得修正后的水平峰值承载力 $P_{uc}(T)$ 计算公式:

$$P_{uc}(T) = k_0 \frac{(1 - 0.15n_0)M_u}{l - D/2} \quad (6)$$

各工况试件水平承载力计算值见表 4。由表 4 可知,常温试件的现有公式计算值与试验值相对误差不超过 9%,符合工程实践要求,同时也表明常温工况采用现有公式所得的钢管约束混凝土柱极限水平承载力有很好的精度;而在高温和低温工况下,现有公式计算值与试验值相对误差最大可达 21.73%。因此,需要考虑环境温度作用,基于已有公式对钢管约束混

土柱水平承载力计算公式予以修正。

表4 不同公式计算值与试验值对比

Tab. 4 Comparison of calculated values of different formulas and experimental values

| 试件编号 | P_u | | 相对误差/% | | |
|------------|-------|---------|---------|--------|-------|
| | 试验值 | 式(3)计算值 | 式(6)计算值 | 式(3) | 式(6) |
| NT-0.3-C60 | 30.60 | 29.30 | 31.29 | -4.24 | 2.26 |
| NT-0.3-C50 | 28.95 | 27.00 | 28.83 | -6.74 | -0.40 |
| NT-0.3-C40 | 28.41 | 26.10 | 27.87 | -8.13 | -1.89 |
| HT-0.3-C60 | 29.30 | 29.30 | 30.23 | -0.01 | -3.20 |
| HT-0.3-C50 | 28.45 | 27.00 | 27.86 | -5.10 | -2.07 |
| HT-0.3-C40 | 27.85 | 26.10 | 26.93 | -6.28 | -3.29 |
| LT-0.3-C60 | 35.36 | 29.30 | 36.39 | -17.13 | 2.92 |
| LT-0.3-C50 | 34.00 | 27.00 | 33.53 | -20.59 | -1.37 |
| LT-0.3-C40 | 33.34 | 26.10 | 32.41 | -21.73 | -2.79 |

注:相对误差=(计算值-试验值)/试验值 \times 100%。

为了验证式(6)对不同温度试件水平承载力计算的精确性,采用文献[41]的试验值、本文试验值与本文式(6)的计算值进行对比验证,验证结果如图12所示。

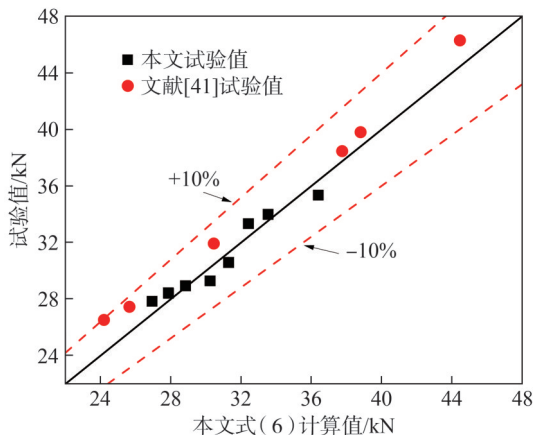


图12 试验值与计算值对比

Fig. 12 Comparison of experimental and calculated results

由图12可知:本文拟合修正公式计算值与本文试验值总体吻合良好,相对误差小于均5.0%;与文献[41]的试验值相对误差均小于10.0%。这表明修正公式具有较高的计算精度,说明本文公式对不同环境温度下试件水平峰值承载力的修正有高度的精确度和合理性。

5 结论

1)钢管约束混凝土柱在不同工况下均为整体压弯破坏,伴有明显的破坏现象。相较于常温工况,低温工况下的试件发生破坏更早且破坏更严重;各试件滞回曲线均呈梭形,无明显捏缩现象,表现出良好的变

形和耗能能力,但低温工况下由于过早破坏,累计耗能相较于常温工况显著减小。

2)环境温度对试件水平承载力和延性均有不同程度的影响,相较于常温工况,低温(-40℃)工况下,试件初始刚度有所增大,峰值承载力最大提高了20.88%,而延性系数最大降低37.52%;高温(60℃)工况下,试件初始刚度有所减小,峰值承载力最大降低4.25%,延性系数最大降低5.27%。

3)钢管约束混凝土柱在不同环境温度下的延性较常温均有所下降,但高、低温环境下的下降机理并不相同。低温环境下由于核心混凝土脆性增加,累积损伤加速发展,使得柱延性显著下降;而高温环境下,主要是由于钢-混凝土界面黏结性能下降,外钢管对核心混凝土的约束效应显著降低所致。

4)本文提出了考虑环境温度影响的钢管约束混凝土柱水平承载力计算修正公式,公式计算值与试验值相对误差小于10%,吻合良好,可为高寒地区该类结构设计提供必要参考。

参考文献:

- [1] 周绪红,刘界鹏,王宣鼎.钢管约束混凝土结构[M].北京:科学出版社,2023.
- [2] Wang Li, Pan Qiren, Zhou Xiaofu, et al. Study on combined effects of bridge temperature and seismic actions based on F-J-M method[J]. Journal of Disaster Prevention and Mitigation Engineering, 2024, 44(2): 273-282. [王力,潘启仁,周晓夫,等.基于F-J-M法的桥梁温度与地震作用效应组合研究[J].防灾减灾工程学报,2024,44(2):273-282.]
- [3] Wang Li, Yu Lusong, Liu Shizhong, et al. Effect of extreme temperatures on seismic response of continuous girder bridge in cold and high-seismicity area[J]. Bridge Construction, 2022, 52(2): 89-96. [王力,虞庐松,刘世忠,等.极端温度对高寒高烈度区连续梁桥地震响应的影响[J].桥梁建设,2022,52(2):89-96.]
- [4] Yu Lusong, Liu Biao, Wang Li, et al. Experimental study on axial compression performance of CFST stub columns under high-cold ambient temperature[J]. Journal of Civil Engineering, 2023, 56(10): 20-31. [虞庐松,刘彪,王力,等.高寒环境温度下圆钢管混凝土短柱轴压性能试验研究[J].土木工程学报,2023,56(10):20-31.]
- [5] Wang Li, Yang Xijuan, Li Ziqi, et al. Experimental study on the interfacial bonding performance of concrete-filled steel tubes at different ambient temperatures[J]. Thin-Walled Structures, 2024, 205: 112368.
- [6] Wang Qiuwei, Jing Xuanguang, Shi Qingxuan, et al. Seismic behavior of steel tubed reinforced concrete column joints with lead viscoelastic dampers[J]. Journal of Vibration and Shock, 2024, 43(6): 238-247. [王秋维,景烜光,史庆轩,等.

- 铅黏弹性阻尼器增强钢管约束钢筋混凝土柱节点抗震性能研究[J]. 振动与冲击, 2024, 43(6): 238–247.]
- [7] Wang Qiuwei, Jing Xuanguang, Jing Ruiying. Seismic performance of steel tube-reinforced concrete column joints embedded with built-in section steel[J]. Journal of Disaster Prevention and Mitigation Engineering, 2024, 44(4): 849–858. [王秋维, 景烜光, 景瑞颖. 内置型钢增强钢管约束钢筋混凝土柱节点抗震性能研究[J]. 防灾减灾工程学报, 2024, 44(4): 849–858.]
- [8] Dai Yan, Nie Shaofeng, Zhou Tianhua. Seismic behavior of circular steel tube-confined H-steel reinforced concrete column–steel frame ring beam joint[J]. Journal of South China University of Technology (Natural Science Edition), 2019, 47(5): 110–122. [戴岩, 聂少锋, 周天华. 环梁式圆钢管约束 H 型钢混凝土柱–钢梁节点的抗震性能[J]. 华南理工大学学报(自然科学版), 2019, 47(5): 110–122.]
- [9] Nie Shaofeng, Ye Mengna, Wu Yangfan, et al. Seismic behavior of square tube confined steel-reinforced concrete column–RC ring beam joint[J]. Journal of Architecture and Civil Engineering, 2019, 36(2): 84–91. [聂少锋, 叶梦娜, 武杨凡, 等. 方钢管约束型钢混凝土柱–RC 环梁节点抗震性能[J]. 建筑科学与工程学报, 2019, 36(2): 84–91.]
- [10] Liu Jian, Mao Jie, Chen Yuan, et al. Seismic behavior of steel recycled concrete column and steel beam joint of square steel tube[J]. Journal of Architecture and Civil Engineering, 2018, 35(3): 25–34. [刘坚, 毛捷, 陈原, 等. 方钢管约束型钢再生混凝土柱–钢梁节点抗震性能分析[J]. 建筑科学与工程学报, 2018, 35(3): 25–34.]
- [11] Bu Shuangshuang, Yu Feng, Chen Taiyao, et al. Experimental study on seismic behavior of circular steel tube confined reinforced self-stressing steel slag concrete columns[J]. Structural Concrete, 2023, 24(1): 1102–1117.
- [12] Zhou Xuhong, Liu Jiepeng, Zhang Sumei. Seismic behavior and strength of tubed SRC beam-columns filled with high strength concrete[J]. China Civil Engineering Journal, 2010, 43(9): 1–11. [周绪红, 刘界鹏, 张素梅. 钢管约束型钢高强混凝土压弯构件的抗震性能研究[J]. 土木工程学报, 2010, 43(9): 1–11.]
- [13] Zang Xingzhen, Yang Yuanlong, Xu Chuangze. Hysteretic behaviors of stiffened T-shaped steel tuber confined concrete columns[J]. Earthquake Engineering and Engineering Dynamics, 2017, 37(5): 129–138. [臧兴震, 杨远龙, 徐创泽. 加劲 T 形钢管约束混凝土柱滞回性能研究[J]. 地震工程与工程振动, 2017, 37(5): 129–138.]
- [14] Xu Li, Hu Hongsong, Peng Biao, et al. Seismic performance of composite jacket-confined square high-strength concrete-filled steel tube columns[J]. Journal of Constructional Steel Research, 2023, 211: 108128.
- [15] Chen Zhihua, Dong Shaohua, Du Yansheng. Experimental study and numerical analysis on seismic performance of FRP confined high-strength rectangular concrete-filled steel tube columns[J]. Thin-Walled Structures, 2021, 162: 107560.
- [16] Feng Peng, Cheng Shi, Yu Tao. Seismic performance of hybrid columns of concrete-filled square steel tube with FRP-confined concrete core[J]. Journal of Composites for Construction, 2018, 22(4): 04018015.
- [17] Ou Zhijing, Cao Lei, Xue Wenhao. Research on seismic performance of square-steel-tube-constrained, prefabricated segmental concrete piers with hybrid joints[J]. Bridge Construction, 2023, 53(1): 40–47. [欧智菁, 曹磊, 薛文浩. 混合接头装配式方钢管约束混凝土桥墩抗震性能研究[J]. 桥梁建设, 2023, 53(1): 40–47.]
- [18] Wang Yuhang, Wang Wei, Zhou Xuhong, et al. Experimental study on seismic behavior of steel tube confined reinforced concrete columns subjected to combined compression–bending–torsion[J]. Journal of Building Structures, 2017, 38(S1): 185–189. [王宇航, 王维, 周绪红, 等. 压–弯–扭耦合荷载作用下钢管约束钢筋混凝土柱抗震性能试验研究[J]. 建筑结构学报, 2017, 38(S1): 185–189.]
- [19] Wang Jingfeng, Hua Zhengmao, Shen Qihan, et al. Experimental and numerical study on seismic performance of elliptical concrete-filled steel tubular columns[J]. China Civil Engineering Journal, 2023, 56(6): 38–51. [王静峰, 华正茂, 沈奇罕, 等. 椭圆钢管混凝土柱抗震性能试验与分析[J]. 土木工程学报, 2023, 56(6): 38–51.]
- [20] Wang Jingfeng, Wang Haitao, Wang Donghua, et al. Experimental study on CFST column-to-steel beam frames with high-strength blind-bolted endplate connections under pseudo-static loading[J]. China Civil Engineering Journal, 2017, 50(4): 13–20. [王静峰, 王海涛, 王冬花, 等. 钢管混凝土柱–钢梁单边高强螺栓端板连接框架的拟静力试验研究[J]. 土木工程学报, 2017, 50(4): 13–20.]
- [21] Shi Yanli, Ji Sunhang, Wang Wenda, et al. Study on hysteretic behavior of tapered concrete-filled double skin steel tubular beam-columns with large hollow ratio[J]. China Civil Engineering Journal, 2022, 55(1): 75–88. [史艳莉, 纪孙航, 王文达, 等. 大空心率圆锥形中空夹层钢管混凝土压弯构件滞回性能研究[J]. 土木工程学报, 2022, 55(1): 75–88.]
- [22] Yan Jiabao, Xie Wenjun, Luo Yanli, et al. Behaviours of concrete stub columns confined by steel tubes at cold-region low temperatures[J]. Journal of Constructional Steel Research, 2020, 170: 106124.
- [23] Yan Jiabao, Xie Wenjun, Zhang Lingxin, et al. Bond behaviour of concrete-filled steel tubes at the Arctic low temperatures[J]. Construction and Building Materials, 2019, 210: 118–131.
- [24] Yan Jiabao, Yang Xinyan, Luo Yunbiao, et al. Studies on axial compression behaviors of concrete-filled steel tubu-

- lar columns at low temperature[J]. *Journal of Building Structures*,2021,42(S2):248–255.[严加宝,杨鑫炎,罗云标,等. 钢管混凝土柱低温轴压性能研究[J]. *建筑结构学报*,2021,42(S2):248–255.]
- [25] Yan Jiabao,Wang Zirui,Luo Yunbiao. Study on eccentric compression performance of ultra-high performance concrete-filled stainless steel tube composite columns in low-temperature environments[J]. *Journal of Building Structures*,2025,46(2):132–140.[严加宝,王子瑞,罗云标. 低温环境下圆不锈钢管UHPC组合柱压弯性能研究[J]. *建筑结构学报*,2025,46(2):132–140.]
- [26] Wang Fengqin,Liu Faqi,Tan Kanghai, et al. Fire test and simulation of circular steel tube confined steel-reinforced concrete columns[J]. *Thin-Walled Structures*,2024,200:111942.
- [27] Wang Fengqin,Liu Faqi,Tan Kanghai, et al. Post-fire performance of circular steel tube confined steel-reinforced concrete slender columns: Testing, simulation and design[J]. *Engineering Structures*,2024,298:117084.
- [28] Wang Fengqin,Liu Faqi,Yang Hua, et al. Axial compressive performances of thin-walled steel tube confined steel-reinforced concrete columns after fire exposure[J]. *Thin-Walled Structures*,2023,190:110919.
- [29] Zhang Ruizhi,Liu Jiepeng,Wang Weiyong, et al. Fire behaviour of thin-walled steel tube confined reinforced concrete stub columns under axial compression[J]. *Journal of Constructional Steel Research*,2020,172:106180.
- [30] Song Tianyi,Tao Zhong,Han Linhai, et al. Bond behavior of concrete-filled steel tubes at elevated temperatures[J]. *Journal of Structural Engineering*,2017,143(11):04017147.
- [31] Parsa-Sharif M,Nematzadeh M,Bahrami A. Post-fire load-reversed push-out performance of normal and lightweight concrete-filled steel tube columns: Experiments and predictions[J]. *Structures*,2023,51:1414–1437.
- [32] Ke Xiaojun, An Jin, Su Yisheng, et al. Experimental study on seismic performance of recycled aggregate concrete-filled square steel tube column after high temperature[J]. *Journal of Experimental Mechanics*,2018,33(6):885–892.
- [柯晓军,安进,苏益声,等. 高温后方钢管再生混凝土柱抗震性能试验研究[J]. *实验力学*,2018,33(6):885–892.]
- [33] Yu Lusong,Wang Geng,Wang Li, et al. Experimental study on the seismic performance of concrete-filled steel tubular columns under ambient temperature in alpine regions[J]. *China Earthquake Engineering Journal*,2024,46(6):1251–1258.[虞庐松,王庚,王力,等. 高寒环境温度下钢管混凝土柱抗震性能试验研究[J]. *地震工程学报*,2024,46(6):1251–1258.]
- [34] 国家质量监督检验检疫总局,中国国家标准化管理委员会. 金属材料 拉伸试验 第 1 部分:室温试验方法:GB/T 228.1—2021[S]. 北京:中国标准出版社,2021.
- [35] 钢与钢产品力学性能试验用试块和试样的位置与制备:GB/T 2975—2018[S]. 北京:中国标准出版社,2018.
- [36] 中华人民共和国住房和城乡建设部,国家市场监督管理总局. 混凝土物理力学性能试验方法标准:GB/T 50081—2019[S]. 北京:中国建筑工业出版社,2019.
- [37] 中华人民共和国住房和城乡建设部. 建筑抗震试验规程:JGJ/T 101—2015[S]. 北京:中国建筑工业出版社,2015.
- [38] Huang Yue,Zhao Pengtuan,Lu Yiyan, et al. Hysteresis performance of steel fiber-reinforced high-strength concrete-filled steel tube columns[J]. *Journal of Constructional Steel Research*,2024,219:108755.
- [39] Yu Qing,Tao Zhong,Chen Zhibo, et al. Flexural behavior of steel tube confined concrete members under pure bending[J]. *Engineering Mechanics*,2008,25(3):187–193.[于清,陶忠,陈志波,等. 钢管约束混凝土纯弯构件抗弯力学性能研究[J]. *工程力学*,2008,25(3):187–193.]
- [40] 韩林海. 钢管混凝土结构——理论与实践[M]. 4 版. 北京:科学出版社,2024.
- [41] Wang Li,Pan Qiren,Gu Haowei, et al. Quasi-static tests of steel tube confined concrete columns considering environmental temperature[J]. *Journal of Vibration and Shock*,2025,44(5):155–168.[王力,潘启仁,顾皓玮,等. 考虑环境温度的钢管约束混凝土柱拟静力试验研究[J]. *振动与冲击*,2025,44(5):155–168.]

Experimental Study on the Influence Mechanism of Ambient Temperature on the Seismic Performance of Steel Tube Confined Concrete Columns

WANG Li¹, HU Qi¹, PAN Qiren¹, GU Haowei¹, ZHAI Qiyuan², YU Lusong¹, KANG Ercong³

(1. School of Civil Engineering, Lanzhou Jiaotong University, Lanzhou 730070, China;

2. Shanxi Jiaoyuan Testing Co., Ltd., Taiyuan 030000, China;

3. School of Civil Engineering, Tianjin University, Tianjin 300350, China)

Abstract:

Objective Steel tube confined concrete (STCC) columns have an increasingly broad application prospect in high-cold and high-intensity areas. In steel-concrete composite structures, the cooperative behavior of steel and concrete is an essential prerequisite for the normal stress performance of such structures. However, due to the influence of ambient temperature on the mechanical properties of steel and concrete and the interaction at their interface, the seismic performance of the structure cannot be ignored. Therefore, to investigate the influence of ambient temperature on the seismic per-

formance of steel tube confined concrete columns, quasi-static tests of steel tube confined concrete columns under different ambient temperatures are conducted. Based on the test results, the influence of ambient temperature on the seismic indices of the specimens is analyzed, and the underlying mechanism by which ambient temperature affects the seismic performance of steel tube confined concrete columns is revealed. In addition, a modified formula for calculating the horizontal bearing capacity of steel tube confined concrete columns considering temperature effects is proposed to provide a necessary basis for the seismic design of steel tube confined concrete structures in high-cold and high-intensity areas.

Methods A set of quasi-static test devices suitable for different ambient temperatures was designed and developed. Quasi-static tests on nine steel tube confined concrete columns were conducted, with ambient temperature and concrete strength selected as the primary research parameters. Comparative tests were performed on three groups of steel tube confined concrete columns under different environmental temperature conditions ($-40\text{ }^{\circ}\text{C}$, $20\text{ }^{\circ}\text{C}$, and $60\text{ }^{\circ}\text{C}$) and three groups with different concrete strengths (C40, C50, and C60). The influence mechanism of ambient temperature on the seismic performance of steel tube confined concrete columns was systematically revealed by comparing and analyzing seismic performance indices, including failure mode, horizontal bearing capacity, ductility performance, stiffness degradation, and energy dissipation capacity of each specimen. Considering the limitation that existing calculation methods for the horizontal bearing capacity of steel tube confined concrete columns did not consider the influence of ambient temperature, the temperature influence coefficient of horizontal bearing capacity was regressed based on the test results in this study. The existing calculation formula for horizontal bearing capacity was multiplied by the temperature influence coefficient k_p , and the accuracy and reliability of the proposed formula were verified through comparisons with the experimental results of this study and other reported test results in the literature.

Results and Discussions The failure modes of specimens under identical temperature conditions were similar and were characterized by typical compression-bending plastic hinge failure. Under all temperature conditions, buckling occurred $10\sim 30\text{ mm}$ above the stiffener at the base of the specimens, with initial local buckling gradually propagating toward both sides. Higher concrete strength resulted in more pronounced local buckling above the stiffener. In addition, steel tube tearing was observed under all temperature conditions. Under normal and high temperature conditions, tearing occurred in the middle of the buckled region, whereas under low temperature conditions, cracks developed along the lower side of the buckle, which was attributed to the significant increase in concrete strength in cold environments. Compared to normal temperature conditions, under low temperature conditions ($-40\text{ }^{\circ}\text{C}$), the initial stiffness and horizontal bearing capacity of the specimens increased by 16.23% and 20.88%, respectively. However, the displacement ductility coefficient decreased by 37.52%, indicating a substantial reduction in ductility and energy dissipation capacity. Under high temperature conditions ($60\text{ }^{\circ}\text{C}$), the initial stiffness and horizontal bearing capacity decreased by 12.52% and 4.25%, respectively, while the displacement ductility coefficient decreased by 5.27%, accompanied by a reduction in energy dissipation capacity. Although increasing concrete strength enhanced horizontal bearing capacity, its overall influence on the seismic performance of steel tube confined concrete columns remained relatively limited. The calculated values obtained using existing formulas showed relative errors of no more than 9% when compared to experimental results under normal temperature conditions, satisfying engineering accuracy requirements. However, under high and low temperature conditions, the maximum relative error between calculated and experimental values reached 21.73%, demonstrating the necessity of considering ambient temperature effects and modifying the existing horizontal bearing capacity calculation formulas accordingly.

Conclusions Ambient temperature has a significant influence on the seismic performance of steel tube confined concrete columns. Ambient temperature and concrete strength exhibit different degrees of influence on the initial stiffness, horizontal bearing capacity, ductility, and energy dissipation capacity of the specimens. These effects are mainly attributed to the additional hoop constraint induced by ambient temperature variations and the corresponding changes in material properties. The ductility of steel tube confined concrete columns under different ambient temperatures is lower than that observed at room temperature; however, the underlying mechanisms of degradation differ. In low-temperature environments, the increased brittleness of the core concrete and the accelerated accumulation of damage lead to a significant reduction in ductility. In high-temperature environments, the reduction in the viscous performance of the steel concrete interface weakens the confinement effect of the outer steel tube on the core concrete, resulting in decreased ductility. A modified formula for calculating the horizontal bearing capacity of steel tube confined concrete columns that considers the influence of ambient temperature is proposed. The relative error between the calculated and experimental values is less than 10%, indicating good agreement and providing a theoretical basis for the design of this type of structure in alpine regions. The design of steel tube confined concrete structures in alpine regions should comprehensively consider the effects of temperature-induced additional confinement and temperature-induced material property changes on the mechanical behavior of the structure.

Key words: steel tube confined concrete column; ambient temperature; quasi-static test; seismic performance; horizontal bearing capacity; temperature-induced additional constraint effects

(编辑 陈雪)

引用格式: Wang Li, Hu Qi, Pan Qiren, et al. Experimental study on the influence mechanism of ambient temperature on the seismic performance of steel tube confined concrete columns[J]. *Advanced Engineering Sciences*, 2026, 58(2): 203–214. [王力, 胡琦, 潘启仁, 等. 环境温度对钢管约束混凝土柱抗震性能影响机理试验[J]. *工程科学与技术*, 2026, 58(2): 203–214.]